Available online on www.ijddt.com
International Journal of Drug Delivery Technology 2018; 8(4); 153-158
doi: 10.25258/ijddt.8.4.1

ISSN: 0975 4415

Research Article

Glucose and Cholesterol Sensing in Blood Plasma Using Zno-Paper Based Microfluidics

Roekmono[1], Harsono Hadi[1], Hilya Nur Imtihani[2], Luthviyah Choirotul Muhimmah[1], Rio Akbar Yuwono[3], Ruri Agung Wahyuono[1*]

[1]*Department of Engineering Physics, Institut Teknologi Sepuluh Nopember, Surabaya, 60111, Indonesia*
[2]*Surabaya Pharmacy Academy, Surabaya, 60232, Indonesia*
[3]*Graduate Institute of Applied Science and Technology, National Taiwan University of Science and Technology, Taipei, 10607, Taiwan*

Received: 7th Mar, 18; Revised: 4th June, 18, Accepted: 8th Nov, 18; Available Online: 25th Dec, 2018

ABSTRACT

This work aims at investigating the reliability of ZnO-paper based microfluidic analytical devices (ZnO-µPAD) for blood plasma separation as well as bio-sensing of glucose and cholesterol. Two-layer paper-based microfluidic analytical devices coated with ZnO nanoflowers/ZnO spherical aggregates (ZnO-µPAD) for a rapid blood plasma separation and glucose sensing were developed. Plasma separation in ZnO-µPAD was evaluated experimentally and numerically using computational fluid dynamics package for a flow over porous networks. Glucose and cholesterol detection was carried out using spectroscopic techniques, both Fourier-transform infrared (FTIR) and Raman measurements. The plasma separation process on ZnO NF-µPAD requires 250 s. The spectroscopic investigation reveals that the IR absorptions and Raman signals at the typical vibrational frequencies of glucose and cholesterol are increasing at higher concentration. After subtraction from absorption background arising from ZnO and the paper, a specific and linearly increasing IR absorption (913 and 1349 cm^{-1}) and Raman signals (1346 and 1461 cm^{-1}) are observable with a relatively good sensitivity.

Keywords: Paper-based microfluidic, ZnO, glucose, cholesterol, FTIR, Raman.

INTRODUCTION

Researchers widely developed paper-based microfluidic devices since it is inexpensive, flexible, light-weight and environmentally friendly[1]. Paper-based microfluidic devices are being exploited in a wide range of applications, including clinical diagnostics, sensing, and energy system[1-3]. In case of clinical diagnostics, paper-based microfluidic analytical devices (µ-PADs) offer a cheap alternative-platform for blood plasma separation and point-of-care diagnosis[1-4]. Typical plasma separation used centrifuge which is less time-efficiency and requires at quite large blood sample volume. Furthermore, existing clinical diagnostic measurements need expensive instruments and advance knowledge for analysis[1-6]. Nowadays, several handheld blood-analyzers were commercialized; it used only small blood sample volume and also does the analyzing in short time. Handheld blood-analyzers were used worldwide by people, but it did not provide the blood plasma separation. As reported by Songjaroen et al[6], blood plasma separation is necessary for some clinical diagnostic to avoid the cells interference during analytical measurements.

Songjaroen at 2012 reported µPADs, with overlapped Whatman No.1 filter paper and Whatman LF-1 paper, can be used for blood plasma separation with widely range hematocrit level[6]. The Whatman no.1 filter paper was used since it is high plasma penetration, while Whatman LF-1 blood separation paper can be used to remove particles greater than 2 – 3 µm[7-9]. Some advancement in µPADs have been made to enhance µPAD potential of clinical diagnosis performance[10-14], and also make it cheaper than using Whatman LF-1 paper, by integrating µPAD using ZnO spherical aggregates (SPs)[7,8]. ZnO can be integrated with the microfluidic device (ZnO-µPAD) since ZnO has high biocompatibility, rapid electron mobility as a biosensor, and allowing immobilizing enzymes with high efficiency via electrostatic attraction[7-9,12,13]. Well-ordered porous matrix and a high surface area of ZnO SPs also make it a good alternative to change Whatman LF-1 paper. ZnO-µPAD well-shown blood plasma separation and successfully performed some clinical diagnostic[8,9,13]. However, it is unclear perform the fast blood plasma separation to provide the time-efficiency. Increasing ZnO-µPAD performance is the main challenge. ZnO nanowires, ZnO nanorods, and ZnO SPs already reported as integrating ZnO-µPAD agent[7-9,10,12,13]. Other ZnO morphology is interesting to integrate with ZnO-µPAD. In this work, ZnO nanoflowers (NFs) in combination with ZnO SPs are utilized for coating paper-based microfluidic (ZnO-µPAD). The resulting ZnO-µPADs is used for separating blood plasma and later used for sensing the glucose and cholesterol level by using different spectroscopic technique.

Author for Correspondence: ruri.tf014@gmail.com

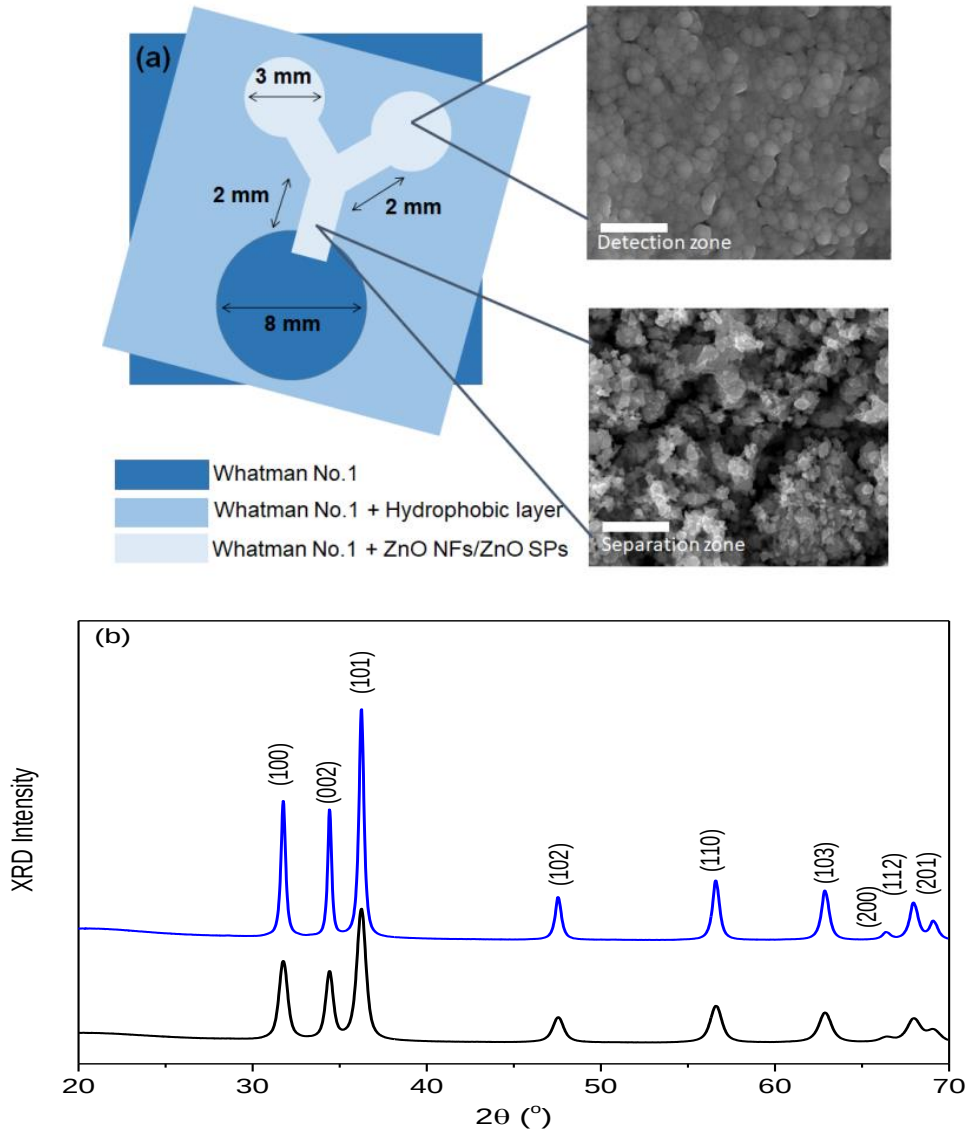

Figure 1: (a) Geometrical design of ZnO-µPAD coated with ZnO nanostructures: ZnO nanoflowers (NFs) and ZnO spherical aggregates (SPs) were deposited on the bottom and top layer, respectively. (b) XRD pattern of ZnO NFs (blue) and ZnO SPs (black).

MATERIALS AND METHOD

Chemicals and Materials

The chemicals were $Zn(CH_3COO)_2{\cdot}2H_2O$, $Zn(NO_3)_2{\cdot}4H_2O$, diethylene glycol (DEG), hexamethylenetetramine (HMTA), ammonia solution, absolute ethanol (etOH). All chemicals were used without purification unless otherwise stated. The materials used were Whatman filter paper grade 1 (pore size 11 µm, filter limit 150 sec/100 mL speed (Herzberg)). The blood samples were collected (Ultra Medica Clinical Laboratory) and characterized with the average dynamic viscosity (μ) and density of blood plasma (ρ) of 1.65×10^{-5} kg·m^{-1}·s^{-1} and 1025 kg·m^{-3}, respectively.

Synthesis and Characterization of ZnO

ZnO nanoflowers (NFs) were synthesized according to our previous synthetic protocol with a slight modification[15-17]: 10 mM $Zn(NO_3)_2{\cdot}4H_2O$ and 10 mM HMTA were dissolved in 500 mL deionized water. The solution was heated at 50°C and stirred for 30 mins. Afterwards, 5 mM KOH solution was added dropwise under vigorous stirring until its pH value reached 10. Finally, the reaction solution was continuously stirred and heated at 90°C for 1 h. The resulting white precipitates were collected, washed several times with distilled water, and then dried under ambient atmosphere. ZnO spherical aggregates (SPs) were prepared according to literature[18-20]: 0.1 M $Zn(CH_3COO)_2{\cdot}2H_2O$ in DEG was heated and stirred at 180°C. The resulting milky solution was centrifuged to separate the ZnO and the supernatant. Both ZnO NFs and ZnO SPs were annealed at 400°C to obtain high crystallinity of ZnO. The microstructural properties of ZnO NFs were measured by X-ray diffraction measurement (XRD X-pert MPD). The diffractometer was operated at 40kV and 20mA using a Cu-Kα radiation. The micromorphology of ZnO NFs was analyzed by Scanning Electron Microscopy (SEM) FEI Inspect-S50 operating at 20.0 kV accelerating voltage.

ZnO-µPAD design

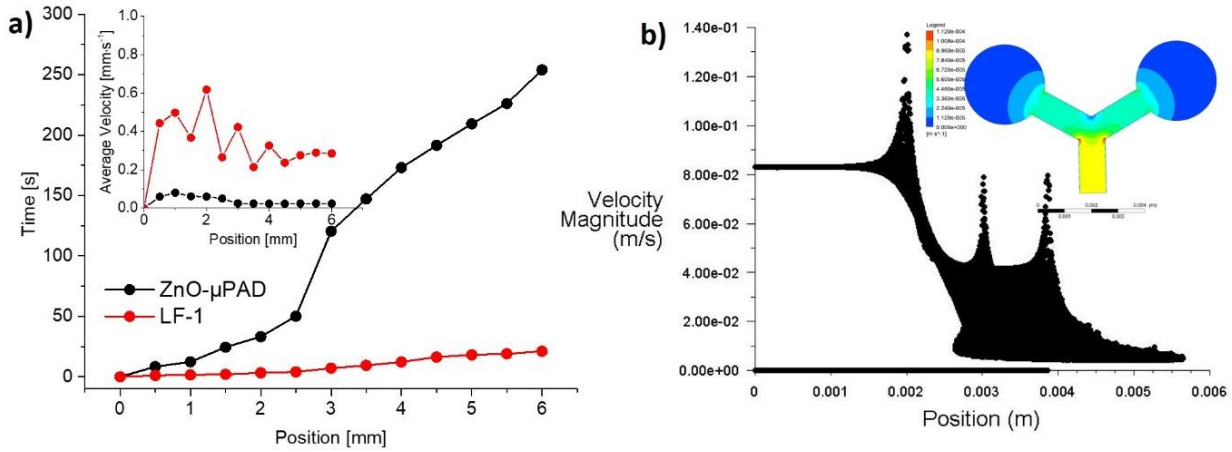

Figure 2: (a) Blood plasma separation profile in ZnO-µPAD including separation time and velocity profile. (b) Velocity magnitude of blood plasma permeated along the microfluidic channels. The inset shows the velocity distribution.

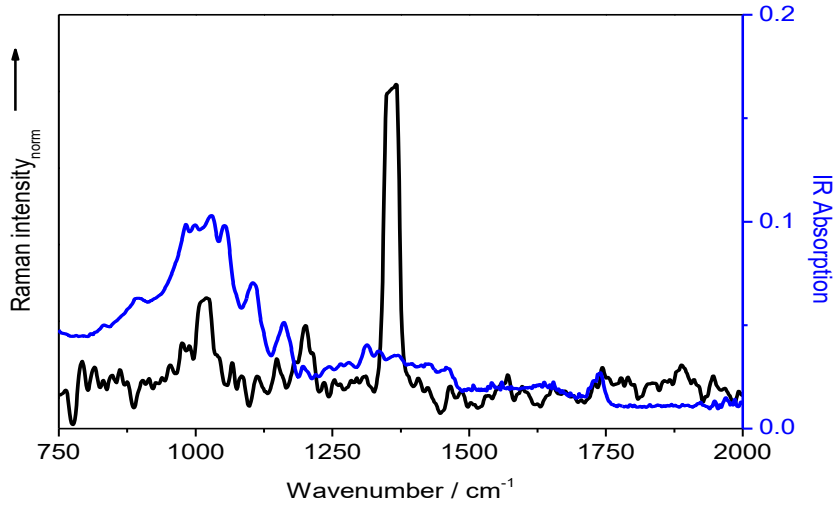

Figure 3: The Raman (black) and IR absorption (blue) spectrum a separated blood plasma in the detection zone of ZnO-µPAD.

In order to increase the separation process, the 3D ZnO-µPAD two-layer were developed. The 2D design in the upper layer was adapted from literature[8]. ZnO-µPAD consisted of two layers of filter paper, the upper of which is perforated (in the sample zone) and covered with ZnO NFs. Eventually, the hydrophobic layer at the border of microfluidic path ways was created by covering with the paraffin wax. The separation channel was coated with ZnO NFs (bottom) and ZnO SPs (top). The flow of blood plasma was induced by the capillary action in the porous networks of filter paper together with ZnO nanostructures. The separation time and velocity of blood plasma was spatially evaluated. In addition, a numerical investigation on the separation mechanism was undertaken by means of computational fluid dynamics (CFD) simulation[8,9,21].

Glucose and Cholesterol measurement

The glucose and cholesterol level of seven samples was evaluated clinically (Ultra Medica Clinical Laboratory). The glucose and cholesterol detection tests of the separated blood plasma were carried out by Fourier-transform infrared (FTIR) measurements (Thermo Scientific Nicolet iS10) within the range of 400 – 4000 cm^{-1}. Raman spectra of separated blood plasma were collected using an electric cooled spectrometer (Raman-HR-TEC, StellarNet) and a diode laser of 120 mW output for excitation at 785 nm. The setup operates via fibres in a 180-degree arrangement and all the measurements were done in triplicate.

RESULTS AND DISCUSSIONS

The ZnO-µPAD design adapted the one reported in literature and has been geometrically optimized prior to the glucose detection according to our previous works. The dimension of ZnO-µPAD is depicted in Fig. 1a. The micromorphology of ZnO NFs at the separation channel and at the detection zone is shown in SEM images. In addition, ZnO NFs-coated filter paper exhibit microporous structure and network for permeation of blood plasma. The microstructural properties of ZnO NFs and ZnO SPs is characterized by XRD pattern shown in Fig. 1b. According to JCPDS card (36-1451), the XRD pattern is assigned as

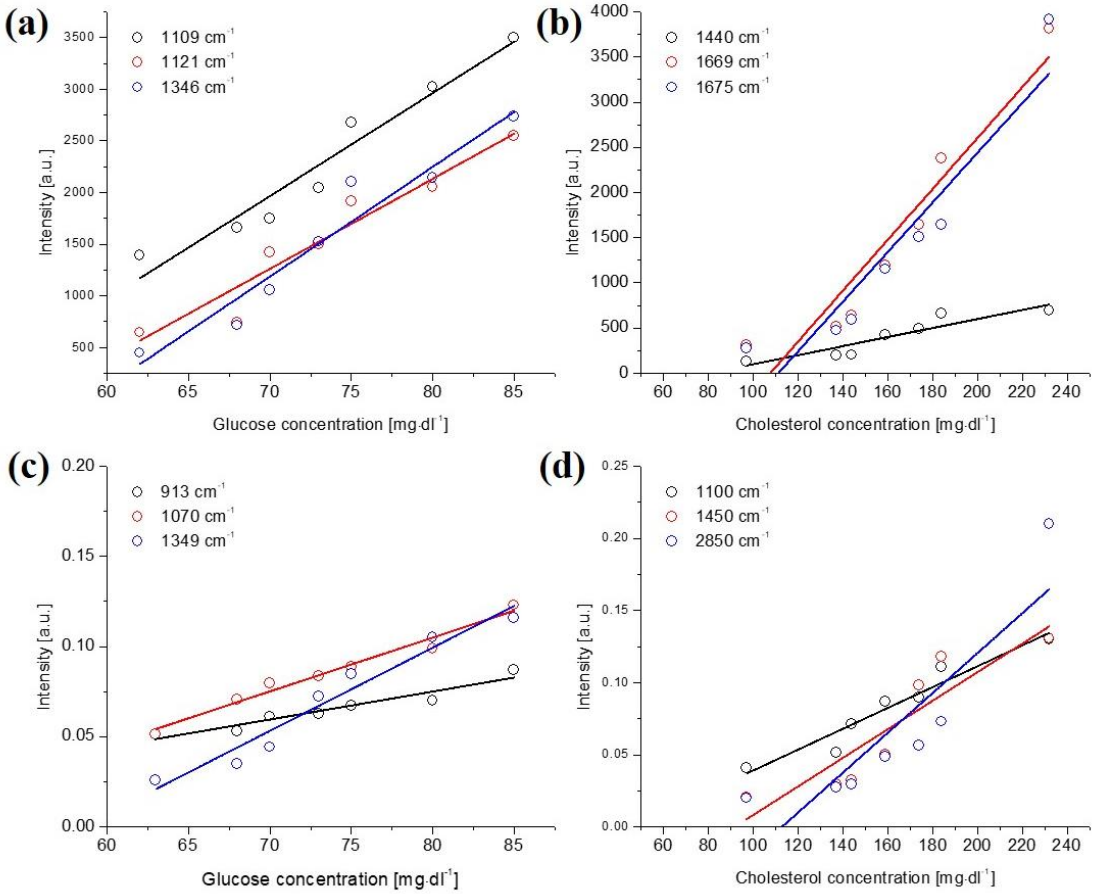

Figure 4: Raman and IR signals of glucose (a,c) and cholesterol (b,d) at selected frequencies. The spectral responses were evaluated after background correction.

hexagonal wurtzite-type, for which the strongest detected (*h k l*) peaks correspond to 2θ values of 31.5°, 34.4° and 36.3° can be assigned to the lattice planes (1 0 0), (0 0 2), (1 0 1), respectively. By using the Debye-Scherer formula, the average crystallite size of ZnO NsF and ZnO SPs calculated from (1 0 1) diffraction peak is 53 and 18 nm, respectively. According to our previous studies[16-18], ZnO NFs and ZnO SPs utilized here possess specific surface area of 11.5 $m^2.g^{-1}$ with unimodal pore distribution and 30 $m^2.g^{-1}$ with bimodal pore distribution, respectively. With a pore volume of 0.035 $cc.g^{-1}$, the ZnO NFs shows porosity of 0.708, viscous resistance (α^{-1}) of 3.6×10^{13} m^{-2}, and inertial resistance (C) of 2.88×10^{6} m^{-1}. Meanwhile, ZnO SPs with a pore volume of 0.134 $cc.g^{-1}$ shows α^{-1} = 2.47×10^{14} m^{-2} and $C_2=5.2\times10^{6}$ m^{-1}. These pore characteristics are useful for numerical investigation below.

The blood plasma separation mechanism is experimentally characterized by the spatially-resolved velocity profile depicted in Fig. 2a. According to the experimental results, the Reynold number (Re) of the blood plasma in ZnO nanostructure is in the order of 10^{-5} and thus characterized as a laminar flow (Re < 3)[22]. In average, the separation time in ZnO-µPAD is ca. 250 s. This separation time is slower than the commercial LF-1 which is possibly due to inhomogeneous ZnO deposition[23]. The velocity magnitude of blood plasma significantly slows down at the junction toward detection zone. Nonetheless, the velocity profile at the detection zone is hardly measured experimentally. The numerical simulation (see Figure 2b) results in a refined profile of the velocity magnitude as well as the dynamic pressure (data not shown). A significant pressure drop at the Y-junction is followed by a decreasing velocity from circa 7.5×10^{-5} to 2.3×10^{-5} $m.s^{-1}$. According to the Darcy and Kozeny-Carman Law, these drops is due to the effect of expanded cross-sectional area of the porous structure. Importantly, the steady-state velocity contour suggests a limited area of separated plasma in the detection zone for bio-sensing.

Having laid the blood plasma separation mechanism in ZnO-µPAD, we turn the discussion on the glucose and cholesterol measurements. The glucose sensing of the separated blood plasma was carried out by FTIR as well as Raman spectroscopy. The IR absorption spectra of the separated blood plasma with different glucose and cholestorl levels (background-corrected, *i.e.* after subtraction with IR absorption of ZnO) are depicted in Fig. 3. The IR bands in the frequency range of 3000 – 2900 cm^{-1} and 2900 – 2800 cm^{-1} are assigned to asymmetric and symmetric valence CH_2 vibrations, respectively, whilst other bands are attributed to the lateral bonds of the C-H pyranose ring[24]. The carbonyl (C=O) stretching vibration is indicated by the spectral peak at 1740 – 1725 cm^{-1}. The infrared bands in the range of 1500 – 1200 cm^{-1} are

Table 1: Static measurement parameters for glucose and cholesterol sensing at selected wavenumbers using Raman and FTIR spectroscopy.

Bio Substance	Method	Wavenumber (cm^{-1})	Sensitivity ($a.u./mg.dl^{-1}$)	Linearity
Glucose	Raman	1109	99.78	0.972
		1121	87.19	0.964
		1346	106.22	0.969
	IR	913	0.0016	0.961
		1070	0.0030	0.987
		1345	0.0046	0.975
Cholesterol	Raman	1440	4.98	0.817
		1667	28.17	0.887
		1675	27.48	0.851
	IR	1100	0.00072	0.965
		1450	0.00099	0.911
		2850	0.00138	0.884

assigned as the deformation vibration of C-H, CH_2 groups as well as C-O-H angles. The bands in the range 1200–950 cm^{-1} are ascribed as the characteristics of the cyclic structure of monosaccharides[24,25]: Valence vibrations of C-O bonds are characterized in the absorption band range of 1200 – 1100 cm^{-1}, whilst mixed vibrations of complex form C-O and C-C bonds are characterized in the absorption range of 1100 – 950 cm^{-1}. The probe frequencies at 1349, 1071, 1020, and 913 cm^{-1} (marked with blue shadows) for IR measurement best indicate the change of □-D-glucose concentration. While probe frequencies at 1100, 1450, 2850 cm^{-1} for IR measurement best indicate the change of cholesterol concentration. For Raman spectra of glucose, it has been identified that glucose exhibits strong Raman signals at 1461, 1346, 1121, and 1109 cm^{-1}, while medium intensity of Raman signals is observed at 1374, 1332, 1273, 1150, 1075, and 1022 cm^{-1} [26]. Nonetheless, we consider merely on the strongest Raman signals at 1346 cm^{-1} and 1461 cm^{-1} for initial probing of different glucose concentration. For cholesterol measurements, Raman signals at 1440, 1669 and 1675 cm^{-1} are the strongest peak to indicate the change of cholesterol concentration.

For analytical devices, the ZnO-µPD should be characterized with not only fast blood plasma separation but also sensitive as well as linear response. Figure 4a and Figure 4b depict the Raman response of separated blood plasma containing different glucose and cholesterol concentrations, while Figure 4c and Figure 4d show the IR absorption response of separated blood plasma containing different glucose and cholesterol concentrations. In general, the obtained data can be fitted with a linear function $y = s\,X + b$, where y is either Raman intensity or IR absorption, s is the slope of linear measurement, X is the concentration of bio substance, and b is the off-set. The resulting static parameters are summarized in Table 1. The slope of the linear fit indicates the sensitivity of the measurement system: IR measurement at 913 cm^{-1} presents higher sensitivity than that at 1349 cm^{-1}, while Raman measurement results in a higher sensitivity at 1346 cm^{-1} than at 1461 cm^{-1}. Even though the linearity of these IR-absorption-based measurements is slightly lower than that reported in our previous study, the development of ZnO NF-µPAD with bilayer papers exhibit promising feature of blood plasma separation without dilution as well as high linearity of glucose concentration measurement system.

CONCLUSION

ZnO-µPADs with a bilayer filter paper enable blood plasma separation directly without further dilution. The separated blood plasma in the detection zone of ZnO-µPADs were characterized with the vibrational spectroscopy to detect the glucose and cholesterol level in the blood plasma. A relatively fast plasma separation (~ 250 s) is achieved and higher blood plasma concentration is accumulated in the mid of detection zone. Measurements using FTIR and Raman spectroscopy results in linear measurement characteristic of glucose and cholesterol with different specificity and high sensitivity. More importantly, this study opens other rooms for optimization toward an efficient blood plasma separation and high performance analytical devices, including the geometrical design of separation channel, the pore structure and volume of ZnO, the deposition method of ZnO colloidal solution, and the sensing/detection method.

ACKNOWLEDGMENT

Financial supports from the research grant of "Penelitian Pemula" (Contract No. 748/PKS/ITS/2017) are gratefully acknowledged.

REFERENCES

1. Martinez AW, Phillips ST, Nie Z, Cheng CM, Carrilho E, Wiley BJ, Whitesides GM. Programmable diagnostic devices made from paper and tape. Lab on a Chip 2010; 10:2499-2504.
2. Riahi R, Tamayol A, Shaegh SAM, Ghaemmaghami AM, Dokmeci MR, Khademhosseini A. Microfluidics for advanced drug delivery systems. Current Opinion in Chemical Engineering 2015; 7:101-112.
3. Li X, Ballerini DR, Shen W. A perspective on paper-based microfluidics: current status and future trends. Biomicrofluidics 2012; 6:011301.
4. Fu YQ, Luo J, Du X, Flewitt A, Li Y, Markx G, Walton A, Milne W. Recent developments on ZnO films for acoustic wave based bio-sensing and microfluidic

applications: a review. Sensors and Actuators B: Chemical 2010; 143:606-619.
5. Fischer C, Fraiwan A, Choi S. A 3D paper-based enzymatic fuel cell for self-powered, low-cost glucose monitoring. Biosensors and Bioelectronics 2016; 79:193-197.
6. Songjaroen T, Dungchai W, Chailapakul O, Henry CS, Laiwattanapaisal W. Blood separation on microfluidic paper-based analytical devices. Lab on a Chip 2012; 12:3392-3398.
7. Yuwono RA, Izdiharrudin MF, Wahyuono RA. Integrated nanoparticles on paper-based microfluidic: toward efficient analytical device for glucose detection based on impedance and FTIR measurement. Second International Seminar on Photonics, Optics, and Its Applications (ISPhOA 2016), International Society for Optics and Photonics, 2016; 10150.
8. Roekmono R, Hadi H, Yuwono RA, Muhimmah LC, Wahyuono RA. deteksi kadar glukosa dalam plasma darah terpisah oleh mikrofluida terintegrasi partikel nano zno berbasis spektroskopi inframerah dan raman. jurnal integrasi proses 2017; 6:148-154.
9. Muhimmah LC, Roekmono, Hadi H, Yuwono RA, Wahyuono RA, Blood Plasma Separation in ZnO Nanoflowers-Supported Paper Based Microfluidic for Glucose Sensing. Proceeding of the 3rd International Conference of Materials and Metalurgical Engineering and Technology (ICOMMET), 30 - 31 October 2017.
10. Tiwari S, Vinchurkar M, Rao VR, Garnier G. Zinc oxide nanorods functionalized paper for protein preconcentration in biodiagnostics. Scientific Reports 2017; 7:43905.
11. Lee JJ, Jeong KJ, Hashimoto M, Kwon AH, Rwei A, Shankarappa SA, Tsui JH, Kohane DS. Synthetic ligand-coated magnetic nanoparticles for microfluidic bacterial separation from blood. Nano letters 2013; 14:1-5.
12. Gallay P, Tosi E, Madrid R, Tirado M, Comedi D. Glucose biosensor based on functionalized ZnO nanowire/graphite films dispersed on a Pt electrode. Nanotechnology 2016; 27:425501.
13. Li X, Zhao C, Liu X. A paper-based microfluidic biosensor integrating zinc oxide nanowires for electrochemical glucose detection. Microsystems & Nanoengineering 2015; 1:15014.
14. Zang D, Ge L, Yan M, Song X, Yu J. Electrochemical immunoassay on a 3D microfluidic paper-based device. Chemical Communications 2012; 48:4683-4685.
15. Iqbal M, Mahendra R, Wahyuono RA, Sawitri D, Risanti DD. Evolution of ZnO Nanoflower-Like Structure Formation and Growth during Synthesis and Paste Preparation. Advanced Materials Research 2015; 1123:219.
16. Wahyuono RA, Schulze B, Rusu M, Wächtler M, Dellith J, Seyring M, Rettenmayr M, Plentz J, Ignaszak A, Schubert US. ZnO Nanostructures for Dye-Sensitized Solar Cells Using the TEMPO+/TEMPO Redox Mediator and Ruthenium (II) Photosensitizers with 1, 2, 3-Triazole-Derived Ligands. ChemPlusChem 2016; 81:1281-1291.
17. Wahyuono RA, Schmidt C, Dellith A, Dellith J, Schulz M, Seyring M, Rettenmayr M, Plentz J, Dietzek B. ZnO nanoflowers-based photoanodes: aqueous chemical synthesis, microstructure and optical properties. Open Chemistry 2016; 14:158-169.
18. Wahyuono RA, Hermann-Westendorf F, Dellith A, Schmidt C, Dellith J, Plentz J, Schulz M, Presselt M, Seyring M, Rettenmeyer M. Effect of annealing on the sub-bandgap, defects and trapping states of ZnO nanostructures. Chemical Physics 2017; 483:112-121.
19. Wahyuono RA. Dye-Sensitized Solar Cells (DSSC) Fabrication with TiO2 and ZnO Nanoparticle for High Conversion Efficiency. Master Thesis, Engineering Physics - ITS, Surabaya, 2013.
20. Wahyuono RA, Risanti DD, Shirosaki T. Photoelectrochemical performance of DSSC with monodisperse and polydisperse ZnO SPs. AIP Conference Proceedings 2014; 1586:78-81.
21. Wibowo ATH, Wahyuono RA, Nugroho G. Studi Numerik Pengaruh Geometri dan Desain Diffuser untuk Peningkatan Kinerja DAWT (Diffuser Augmented Wind Turbine). Jurnal Teknik Mesin 2013; 14:90-96.
22. Ergun S. Fluid flow through packed columns. Chem. Eng. Prog. 1952; 48:89-94.
23. Cao H, Amador C, Jia X, Ding Y. Capillary dynamics of water/ethanol mixtures. Industrial & Engineering Chemistry Research 2015; 54:12196-12203.
24. Korolevich M, Zhbankov R, Sivchik V. Calculation of absorption band frequencies and intensities in the IR spectrum of α-D-glucose in a cluster. Journal of molecular structure 1990; 220:301-313.
25. Vasko PD, Blackwell J, Koenig J. Infrared and raman spectroscopy of carbohydrates: Part I: Identification of O-H and C-H-related vibrational modes for D-glucose, maltose, cellobiose, and dextran by deuterium-substitution methods. Carbohydrate Research 1971; 19:297-310.
26. Shafer-Peltier KE, Haynes CL, Glucksberg MR, Van Duyne RP. Toward a glucose biosensor based on surface-enhanced Raman scattering. Journal of the American Chemical Society 2003; 125:588-593.